

Journal of Materials Chemistry C

Accepted Manuscript



This is an *Accepted Manuscript*, which has been through the Royal Society of Chemistry peer review process and has been accepted for publication.

Accepted Manuscripts are published online shortly after acceptance, before technical editing, formatting and proof reading. Using this free service, authors can make their results available to the community, in citable form, before we publish the edited article. We will replace this *Accepted Manuscript* with the edited and formatted *Advance Article* as soon as it is available.

You can find more information about *Accepted Manuscripts* in the [Information for Authors](#).

Please note that technical editing may introduce minor changes to the text and/or graphics, which may alter content. The journal's standard [Terms & Conditions](#) and the [Ethical guidelines](#) still apply. In no event shall the Royal Society of Chemistry be held responsible for any errors or omissions in this *Accepted Manuscript* or any consequences arising from the use of any information it contains.

ARTICLE

Reduced Efficiency Roll-off in Light-Emitting Diodes Enabled by Quantum Dot-Conducting Polymer Nano hybrids

Cite this: DOI: 10.1039/x0xx00000x

Received 00th January 2012,
Accepted 00th January 2012

DOI: 10.1039/x0xx00000x

www.rsc.org/W. K. Bae,^a J. Lim,^b M. Zorn,^c J. Kwak,^d Y.-S. Park,^b D. Lee,^d S. Lee,^e K. Char,^f
R. Zentel,^c and C. Lee^d

We demonstrate QLEDs implementing wider active layers (50 nm) based on QD-conducting polymer nano hybrids, which exhibit stable operational device performance across a wide range of current density and brightness. A comparative study reveals that the significant suppression of efficiency roll-off in the high current density regime is primarily attributed to the sufficient charge carrier distribution over the wider active layer and improved charge carrier balance within QDs enabled by the hybridization of QDs with conducting polymers. Utilization of this finding in the future studies should greatly facilitate the development of high performance, stable QLEDs at high current density or luminance regime toward displays or solid-state lighting applications.

I. Introduction

Nanocrystal quantum dots (QDs) has drawn keen attentions in light-emitting applications due to their advantageous properties, such as broad absorption but narrow emission, easy emission tunability ranging from UV to near IR, excellent photoluminescent quantum yield (PL QY) and their solution processing capability.¹ Since the first quantum dot-based light-emitting diodes (QLEDs) were demonstrated,² multilateral efforts have been taken to improve device performances.^{3, 4} Recently QLEDs with device performances close to conventional light-emitting devices have been successfully realized (*i.e.*, peak external quantum efficiency (EQE) of 18 %, maximum luminance above 10,000 cd m⁻² and an operational half-lifetime of 1,000 hour at 500 cd m⁻²).⁴

Despite rapid developments, there still remains daunting issues to be solved for their practical usage. The efficiency decrease at high current densities (referred as efficiency roll-off), particularly in the range of applicable brightness, has been considered as one of the most serious device problems, limiting their practical applications toward displays, solid-state lightings and lasers. The origins for the substantial efficiency roll-off in QLEDs, compared with conventional LEDs with a similar device structure (*i.e.*, *p-i-n* structure) and materials, have been suggested as following reasons: 1) the material instability of QDs by Joule heating, 2) decrease in radiative exciton recombination rate under high electrical field⁶ and 3) exciton loss via non-radiative Auger recombination processes.^{7, 8}

While continuing progresses have been made to enhance the single exciton or multicarrier recombination efficiency⁹ as well as the photochemical stability of QDs,¹⁰ the device structure remains indeed same as a *p-i-n* structure with narrow and compact QD active layers (typically, 1-2 monolayers (MLs)). The reason for the limited choice in device architectures is attributed to the poor charge carrier transport property between core/shell structured QDs stabilized with insulating organic surfactants (typically, 1 nm in length). The structural feature of conventional QLEDs seems to inevitably lead higher charge carrier (or exciton) concentrations within individual QDs, and could result in the efficiency roll-off at high current densities due to the exciton loss process *via* Auger recombination process.^{7, 8, 11} This line of reasoning motivates our study of the correlation between the morphology of QD active layers and the performance of QLEDs.

In this study, we for the first time present the comparative study on the influence of QD morphologies to the device performances. To fully realize the morphological contrast of active materials, we prepare QD arrays with improved carrier transport properties by hybridizing QDs with conducting polymer brushes. The systematic comparison of device performance between QLEDs employing active layers with different QD morphologies (~ 8MLs) reveals that the wide QD active layer leads to the reduced efficiency roll-off at high current densities compared with the narrow QD distribution (1-2 MLs) placed on top of a carrier transport layer. We attribute the reason for the reduced efficiency roll-off in QLEDs with

QD-polymer hybrids to the efficient charge distribution across the active layers and the improved charge balance within QDs. In case of QD/conducting polymer hybrids, QDs distribute uniformly within a hybrid matrix and therefore the exciton density across the active emissive layer is lower than the conventional QLED structure, resulting in suppressed exciton loss even at high current densities. Moreover, the electron-hole balance within the QD/conducting polymer hybrid emissive layer can be improved due to the improved carrier injection at the interface between QDs and conducting polymer brushes. As a result, QLEDs exhibiting the stable device efficiency of 1.38 % (Std. = ± 0.03) over the wide range of current density ($1 \sim 200 \text{ mA cm}^{-2}$) as well as color-saturated EL emission (FWHM = 28 nm) with the maximum brightness above $7,000 \text{ cd m}^{-2}$ have been realized. The approaches taken in the present study establish, for the first time, the detailed correlation between the reduced efficiency roll-off in QLEDs and the nanoscopic morphology of QD active layer and thus suggest reasonable guidelines in designing materials and device architectures of QLEDs toward practical applications as full color displays and solid-state lightings.

II. Results and discussion

Various methods have been taken account to improve the carrier transport property within multilayer QD arrays either by removing the surfactants or by replacing them with short hydrocarbon chains or conductive organic/inorganic moieties.¹² Among these plausible approaches, we adopted the hybridization of QDs with conducting polymers^{13, 14} for the present study, not only because of the enhanced carrier transport through the conducting polymer brushes and the facilitated carrier injection/separation at the interface between QDs and conducting polymer brushes, but also due to the improved colloidal stability and the flexible processing capability of the hybrids originating from chemically grafted polymer brushes.

For QLED fabrication, QDs with chemical composition gradient (with a diameter of 8 nm stabilized with oleic acids) synthesized as previously reported methods are used.¹⁰ To replace the insulating oleic acid ligand layer, a block copolymer containing a hole-conducting block was designed based on triphenylamine units. We chose the dimeric TPD derivative with methoxy side groups as substituents in the para-position. These structures are known to be chemically and electrically stable with an improved hole carrier mobility in comparison to the standard TPA, which was used in our previous work.^{13, 14} The synthesized monomer was polymerized through RAFT polymerization (Supporting Information). This hole conducting block (55 repeating units) was used as a macrochain transfer agent to polymerize a second block. We used here a reactive ester species (pentafluorophenolacrylate) which allows a flexible introduction of variable anchor groups (30 rpu). As an anchor unit we used a protected thiol structure to prevent oxidative crosslinking. The anchor unit was synthesized by protection of cysteamine with methyl methanethiosulfonate (MTS). The methylated disulfide binds efficiently to QDs but does not undergo interchain cross linking. The block copolymer (poly(TPD-*b*-SSMe)) was hybridized with the QDs through the *grafting-to* method (Fig. 1a).¹³ TPD, which is widely used in OLEDs as the HTL, was chosen as the conducting moiety in this study due to its chemical and electrical stability. The HOMO and LUMO energy levels of the synthesized poly(TPD-

b-SSMe) were determined to be as 5.6 eV and 2.6 eV, respectively, based on ultraviolet photoelectron spectroscopy (UPS) measurements and UV-visible spectra (see Fig. S3). Even after hybridization of QDs with conducting block copolymers, the QDs maintain their initial optical properties, for example, Gaussian PL emission spectra ($\lambda_{\text{max.}} = 508 \text{ nm}$, FWHM = 28 nm), PL QY of 80 % (excited at 420 nm) and PL decay dynamics (Fig. 1c, 1d), indicating that exciton decay dynamics within QD remain essentially unchanged throughout the hybridization method.

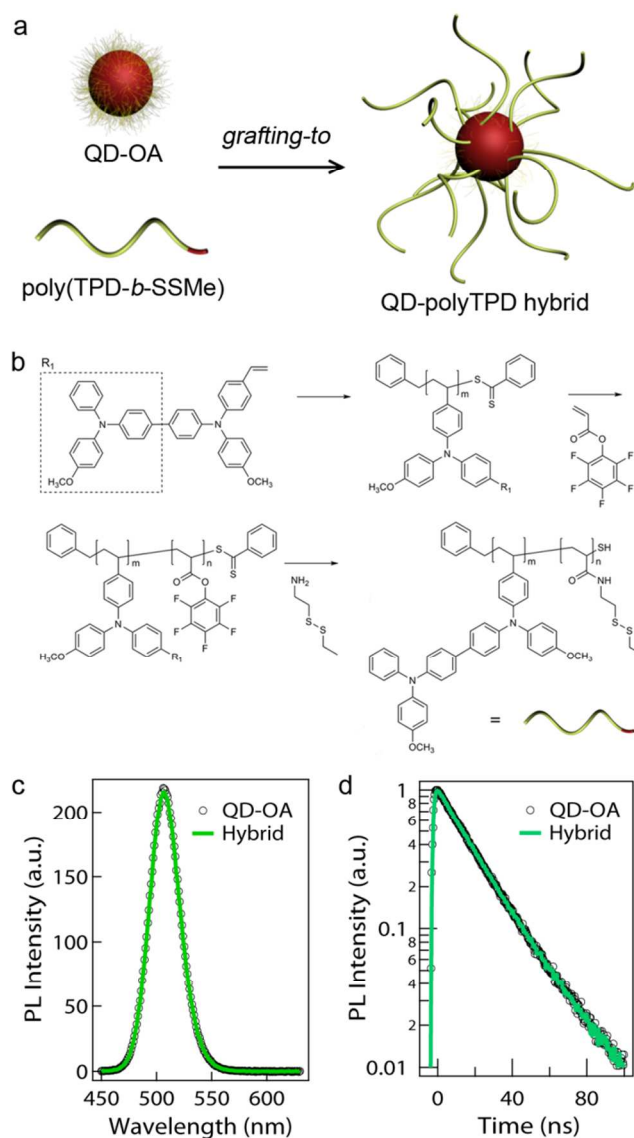


Figure 1. (a) A schematic on the hybridization of QDs (initially stabilized with oleic acids, QD-OA) with poly(TPD-*b*-SSMe) through the *grafting-to* modification method. (b) A synthetic pathway to prepare poly(TPD-*b*-SSMe). Detailed synthetic procedures are provided in Supporting Information. (c) PL spectra and (d) PL decay dynamics of QDs and QD-poly(TPD-*b*-SSMe) hybrids (excited at 405 nm). The single exciton dynamics within QDs are preserved throughout the surface modification process.

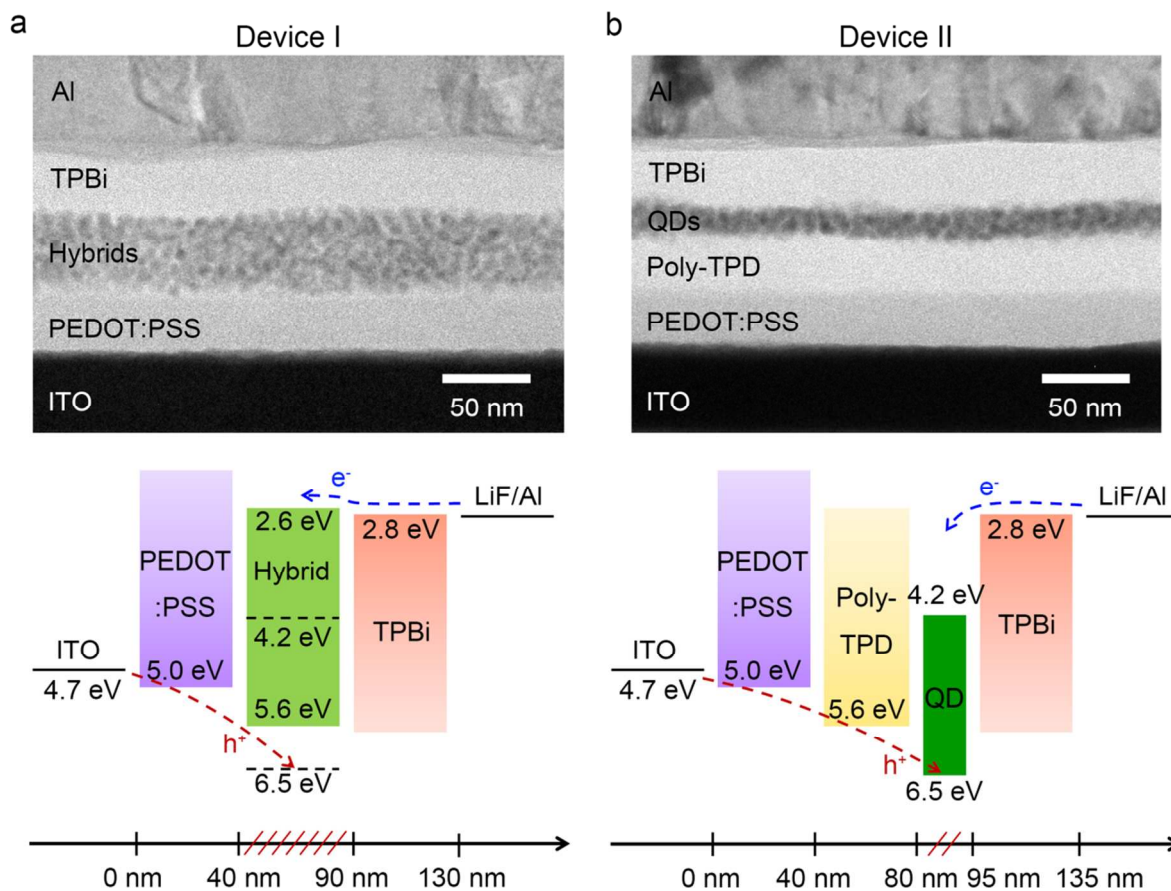


Figure 2. Cross-sectional TEM images and energy band diagrams of (a) QLED employing a QD-poly(TPD-*b*-SSMe) hybrid layer (ca. ~ 8 MLs) as the active layer (Device I) and (b) QLED employing a pristine QD active layer (ca. ~ 1.5 MLs) placed between polyTPD and TPBi (Device II).

To establish the detailed correlation between QD morphology within the active layer and device characteristics, QLEDs containing the QD-poly(TPD-*b*-SSMe) hybrid film (with broad and uniform distribution of QDs within the hybrid layer) as the active layer (Device I, **Fig. 2a**) was designed and compared with the conventionally structured QLEDs employing the compact QD layers (1-2 MLs, with QDs in close contact with each other) placed on the charge transport layer (Device II, **Fig. 2b**). QDs from the same batch and organic charge transport layers with proven stability and performances were employed for both QLEDs to minimize the unexpected influence of materials to the device performances. Both devices were prepared based on a device configuration of ITO (anode) // poly(3,4-ethylenedioxythiophene): poly(styrenesulfonate) (PEDOT:PSS) (40 nm) // active layer ((QD-poly(TPD-*b*-SSMe) hybrid layer (50 nm) (Device I) or poly-(N,N'-bis(4-butylphenyl)-N,N'-bis(phenyl)benzidine) (polyTPD, 40 nm)/ QD (1.5 monolayers) (Device II)) // 1,3,5-tris(N-phenylbenzimidazo 1-2,yl) benzene (TPBi) (40 nm) // LiF (0.5 nm) // Al (100 nm) (cathode). PEDOT:PSS was employed to facilitate the hole injection from ITO to the active layer. TPBi was selected as the electron transporting layer (ETL) as well as the hole blocking layer. The cross-sectional TEM images in **Figure 2** clearly show the QD morphologies in QLEDs. Device I possesses the hybrid active layer (50 nm) with broad and uniform QD distribution within the conducting polymer (*i.e.*,

poly(TPD-*b*-SSMe)) matrix due to energetically favorable attractions between QDs and SSMe anchor blocks. Device II possesses a compact QD emitting layer (with 1.5 QD monolayers with QDs in close contact with each other) placed between charge carrier transport layers (*i.e.*, polyTPD and TPBi). Among the Devices II with different QD thickness (*i.e.*, number of QD monolayers), the QLED (Device II) with 1.5 QD monolayers was chosen for comparison, because it exhibited the best device performance in terms of turn-on voltage, brightness, and external quantum efficiency among same device structures with different QD active layer thickness.¹⁵ The nominal QD density within the active layers are estimated as $5.0 \times 10^{12} \text{ cm}^{-2}$ for Device I and $1.2 \times 10^{12} \text{ cm}^{-2}$ for Device II (see Supporting Information for discussion).

Figure 3 shows the device characteristics (*i.e.*, current (J) – voltage (V) – luminance (L), EL spectrum and external quantum efficiency) of Device I and Device II. Both QLEDs exhibit narrow EL spectra with a Gaussian shape ($\lambda_{\text{max.}} = 510 \text{ nm}$, FWHM = 28 nm) at current densities ranging from 25 mA cm^{-2} to 150 mA cm^{-2} (**Fig. 3b**), which indicates that QDs are indeed the major emitting centers within the active layer for both types of QLEDs. In contrast to the previous report (in the case of the QLED with a QD monolayer placed within HTL (*i.e.*, TPD)), the parasitic emission from the HTL matrix was not observed in Device I, representing the efficient exciton

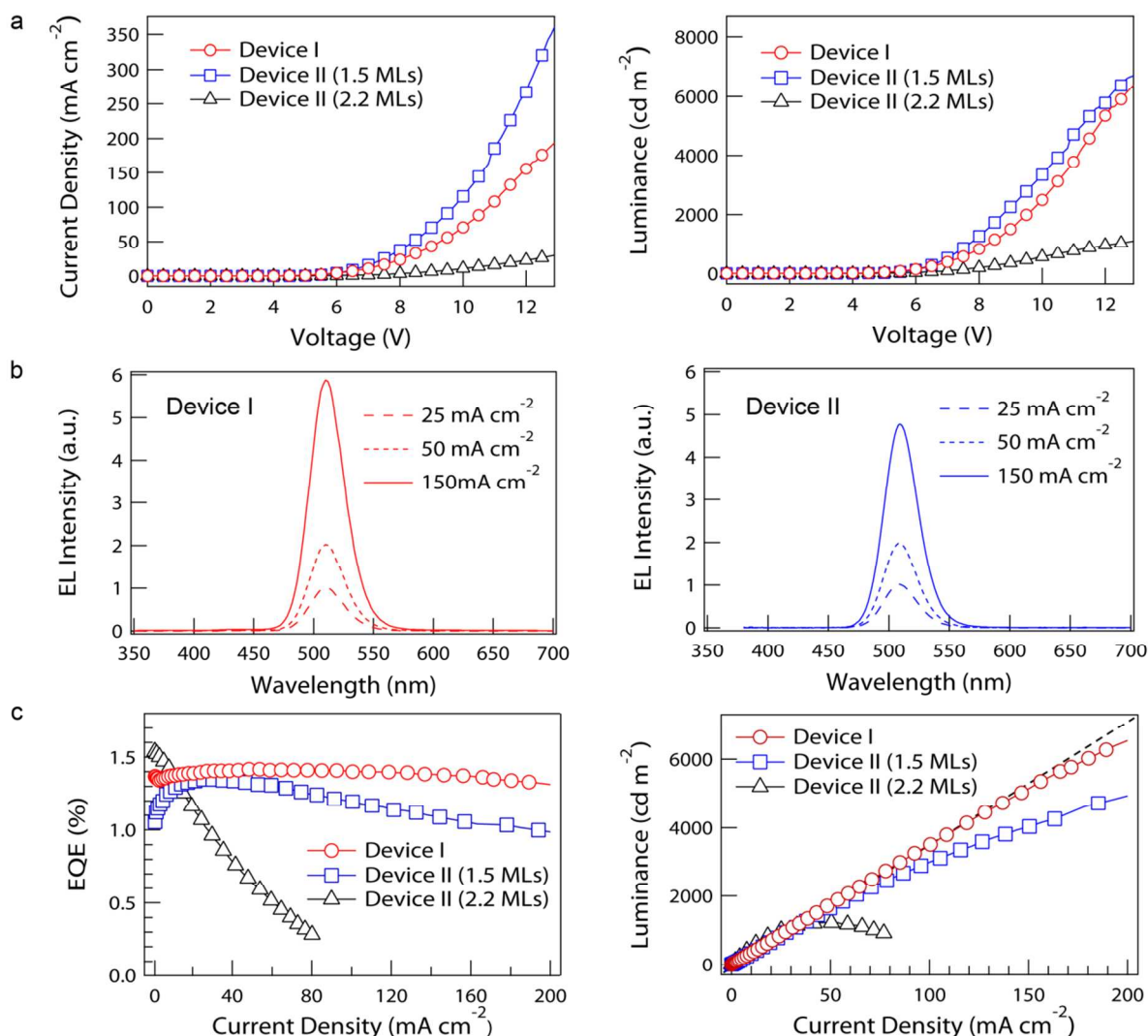


Figure 3. (a) Current (J) – voltage (V) – luminance (L) characteristics, (b) EL spectra, and (c) external quantum efficiency (EQE) – current (J) – luminance (L) characteristics of QLEDs for Devices I and Device II. The dotted guideline (---) in Figure 3c (right) represents the linear increase of luminance along the current density. Note that the Device I exhibits stable device efficiency (Avg. EQE = 1.38 %) over the wide current density (1 ~ 200 mA cm⁻²), while the Device II shows the efficiency roll-off above the current density of 50 mA cm⁻².

formation within QDs enabled by the efficient carrier (electron and hole) injection from poly(TPD-*b*-SSMe) into QDs as well as the enhanced exciton transfer from poly(TPD-*b*-SSMe) to QDs. Although both devices show similar luminance profiles as a function of applied voltage, notable difference could be found in the device efficiency as a function of current densities (Fig. 3c). Device I shows the stable device efficiency (Avg. EQE = 1.38 %, Std.(σ) = \pm 0.03) in current densities ranging from 1 to 200 mA cm⁻², while Device II shows a rather large variation in device efficiency (Avg. EQE = 1.20 %, Std.(σ) = \pm 0.11) and the drastic efficiency roll-off behavior at current densities above 50 mA cm⁻². We also note that the increase in the film thickness of the QD emitting layer for Device II above two QD monolayers does not improve the efficiency roll-off at higher current densities and, instead, causes significantly decrease in the current density and luminance as well as even pronounced efficiency roll-off as a result of insufficient charge carrier transport through the QD multilayer film.

We attribute the significant improvement in the efficiency roll-off behavior of Device I to the QD morphology within the active hybrid layer (*i.e.*, broad and uniform QD distribution within the hole transport matrix (*i.e.*, poly(TPD-*b*-SSMe)). Since QDs possess lower conduction/valence band edge energy levels (\sim 1eV) compared with the LUMO/HOMO energy level of typical conjugated organic molecules or polymers, the electron injection into QDs from the adjacent organic layers (*i.e.*, polyTPD or TPBi) occurs rather spontaneously (which means under little or without applied voltage) while the hole injection takes place only under the assistance of external electric field. Moreover, the mobility of charge carriers within hole/electron transport layers (*i.e.*, polyTPD/TPBi) alters depending on the electrical field, and thus effective exciton recombination zone shifts within the devices strongly depending on the field. In case of conventionally structured QLEDs (Device II) with a thin compact active layer consisting of one or two QD monolayers (ca. QD density: 1.2×10^{12} cm⁻² in present study),

both excitons and charge carriers (particularly electrons) are accumulated within the compact QD arrays in relatively higher concentration at increased current densities, leading to the exciton loss within QDs by the non-radiative Auger recombination process. By contrast, the broad QD active layer within the hole transport layer (Device I, ca. QD density: $5.0 \times 10^{12} \text{ cm}^{-2}$ in present study) enables efficient distribution of charge carriers or excitons and also improve the charge balance within the active layer (particularly by improving the hole injection rate into QD active layers). As a consequence, the device exhibits stable efficiency even at high current densities (electrical field) due to the suppressed exciton loss.

In present study we attribute the improved efficiency roll-off of QLEDs to the broad distribution of charge carriers over QD active layers and the improved charge balance by hybridization of QDs with QD-poly(TPD-*b*-SSMe). Since Auger recombination, which universally occurs in QDs, is known to be responsible for the efficiency roll-off behavior in QLEDs,⁸ we expect that our approach and results in present study can be extended to QLEDs with better efficiency. A clear next step to further improve the device performances is development of new conducting polymer brush layers, which can help balance charge carrier balance in QDs. The reduced hole injection barrier at the interface of conducting polymer and QDs will enhance the charge balance within QDs and improve the device performances. We also believe that, in parallel, multilateral efforts on synthesis of QDs with improved stability and efficiency, optimization of device structures, and better understanding of device operation or degradation mechanism will further improve the device performances, enabling the practical use of QLEDs to displays and lighting applications.

III. Summary

In summary, we presented comparative study on the influence of morphologies of QD active layers to the performances of QLEDs, particularly in terms of efficiency roll-off at high current densities and brightness. To fully realize the morphological contrast, we have prepared QD-conducting polymer hybrids (QD-poly(TPD-*b*-SSMe)) with improved charge carrier properties. In contrast to conventional QLEDs with narrow and compact QD emitting layers (*i.e.*, 1-2 MLs at most) sandwiched between HTL and ETL, QLEDs with broad QD distribution based on QD-poly(TPD-*b*-SSMe) hybrid active layer exhibited stable device operation (reduced efficiency roll-off) in a wide range of current densities, indicating the suppressed exciton quenching within QDs at higher current densities due to efficient distribution of excitons and carriers across the active layer as well as improved charge balance within the active layer. As a result, we could realize QLEDs with a stable device efficiency of 1.38 % (Std. = ± 0.03) in the wide range of current density ($1 \sim 200 \text{ mA cm}^{-2}$) as well as the color-saturated EL emission (FWHM = 28 nm) with the maximum brightness above $7,000 \text{ cd m}^{-2}$. The approaches and the results shown in the present study address, for the first time, the reduced efficiency roll-off in QLEDs in correlation with nanoscopic morphologies of QD active layers and thus suggest reasonable guidelines in designing materials or device architecture of QLEDs toward practical applications as full color displays and solid-state lighting.

Experimental methods

Materials: CdSe@ZnS QDs (with diameter of 8 nm) stabilized with oleic acid were synthesized as previously reported.¹⁰ 100 ml reaction flask containing 0.2 mmol of cadmium oxide, 4 mmol of zinc acetate and 4 ml of oleic acid was degassed under vacuum at 100 °C for 30 min, filled with nitrogen, and heated up to 300 °C. At the elevated temperature, 2 ml of trioctylphosphine dissolving 0.2 mmol of Se and 4 mmol of S were swiftly injected into the reaction flask. The reaction was proceeded for 10 min and cooled down to room temperature. QDs were purified repeatedly (5 times) and dispersed in toluene for further experiment. Poly(TPD-*b*-SSMe) was obtained by the conversion of pentafluorophenol groups in poly(TPD-*b*-PFP) with 2-(2-ethylidysulfanyl)ethanamine. A QD-poly(TPD-*b*-SSMe) hybrid solution was prepared by mixing 0.5 ml of QD dispersion (6 wt% in toluene) with 0.5 ml of poly(TPD-*b*-SSMe) solution (3 wt% in toluene). Detailed synthetic procedures are provided in the Supporting Information.

Device fabrication and characterization: PEDOT:PSS was first spin-cast on a patterned ITO substrate at 4000 rpm for 30 min and baked in a vacuum oven at 120 °C for 30 min. QD-poly(TPD-*b*-SSMe) hybrid film was spun-cast at 4000 rpm for 30 sec and annealed at 80 °C under N₂ atmosphere for 30 min to remove residual solvent. PolyTPD/QD bilayer film was prepared by spin-casting each solution (polyTPD in chlorobenzene (1.5 wt%) and QD in toluene (2 wt%)) consecutively at 4000 rpm for 30 sec. TPBi, LiF and Al were thermally evaporated with deposition rates (monitored with a quartz-oscillator) of $1 - 2 \text{ \AA sec}^{-1}$, 0.1 \AA sec^{-1} , and $4 - 5 \text{ \AA sec}^{-1}$, respectively. The current (J)–voltage (V)–luminance (L) characteristics were measured using a Keithley 236 source-measure unit and a Keithley 2000 multimeter coupled with a calibrated Si photodiode. EL spectra of the devices tested in the present study were obtained with a Konica-Minolta CS-1000A spectroradiometer.

Acknowledgements

This research was financially supported by Korea KIST internal project (2E24821). This work was also financially supported by the National Research Foundation of Korea (NRF) funded by the Korea Ministry of Education, Science, and Technology (MEST) through the the National Creative Research Initiative Center for Intelligent Hybrids (No. 2010-0018290), the Basic Science Research Program (2011-0022716), and Technology Development Program to Solve Climate Changes (No. NRF-2009-C1AAA001-2009-0093282). This work was in part supported by the International Research Training Group: Self Organized Materials for Optoelectronics, jointly supported by the DFG (Germany) and NRF (Korea).

Notes and references

^a Photo-Electronic Hybrids Research Center, National Agenda Agenda Research Division, Korea Institute of Science and Technology, 14-gil 5, Hwarang ro, Seongbuk gu, Seoul 136-791, Korea.

^b Chemistry Division, Los Alamos National Laboratory, New Mexico 87544, United States.

^c Institute of Organic Chemistry, Johannes Gutenberg-Universität Mainz, Duesbergweg 10-14, 55099 Mainz, Germany.

^d Department of Electrical Engineering and Computer Science, Inter-University Semiconductor Research Center (ISRC), Seoul National University, 1 Gwanak-ro, Gwanak-gu, Seoul 151-742, Korea.

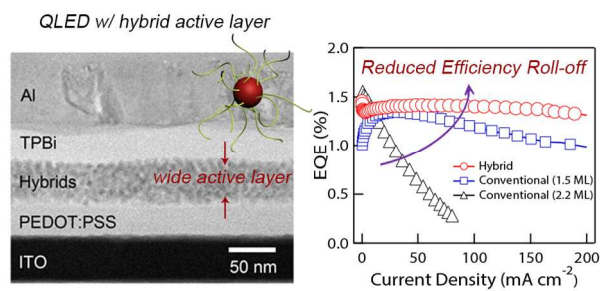
^e Department of Chemistry, Seoul National University, 1 Gwanak-ro, Gwanak-gu, Seoul 151-742, Korea.

^fSchool of Chemical and Biological Engineering, The National Creative Research Initiative Center for Intelligent Hybrids, Seoul National University, 1 Gwanak-ro, Gwanak-gu, Seoul 151-742, Korea.

Electronic Supplementary Information (ESI) available: [Synthetic procedures and optical properties for oleic acid capped QDs and poly(TPD-*b*-SSMe), UPS data for poly(TPD-*b*-SSMe), AFM images and TEM images of oleic acid capped QDs and QD-poly(TPD-*b*-SSMe) nanohybrids, and cross-sectional and plane high resolution TEM images of QD-poly(TPD-*b*-SSMe) hybrid films within devices]. See DOI: 10.1039/b000000x/

1. L. Brus, *J. Phys. Chem.*, 1986, **90**, 2555; A. P. Alivisatos, *Science*, 1996, **271**, 933; V. I. Klimov, *CRC*, 2010, **2nd edn**.
2. V. L. Colvin, M. C. Schlamp and A. P. Alivisatos, *Nature*, 1994, **370**, 354.
3. S. Coe, W.-K. Woo, M. Bawendi and V. Bulovic, *Nature*, 2002, **420**, 800; A. H. Mueller, M. A. Petruska, M. Achermann, D. J. Werder, E. A. Akhadow, D. D. Koleske, M. A. Hoffbauer and V. I. Klimov, *Nano Lett.*, 2005, **5**, 1039; J. M. Caruge, J. E. Halpert, V. Wood, V. Bulovic and M. G. Bawendi, *Nat. Photon.*, 2008, **2**, 247; L. Qian, Y. Zheng, J. Xue and P. H. Holloway, *Nat. Photon.*, 2011, **5**, 543.
4. J. Kwak, W. K. Bae, D. Lee, I. Park, J. Lim, M. Park, H. Cho, H. Woo, D. Y. Yoon, K. Char, S. Lee and C. Lee, *Nano Lett.*, 2012, **12**, 2362.
5. B. S. Mashford, M. Stevenson, Z. Popovic, C. Hamilton, Z. Zhou, C. Breen, J. Steckel, V. Bulovic, M. Bawendi, S. Coe-Sullivan and P. T. Kazlas, *Nat. Photon.*, 2013, **7**, 407.
6. Y. Shirasaki, G. J. Supran, W. A. Tisdale and V. Bulović, *Phys. Rev. Lett.*, 2013, **110**, 217403; D. Bozyigit, O. Yarema and V. Wood, *Adv. Funct. Mater.*, 2013, **23**, 3024.
7. V. I. Klimov, A. A. Mikhailovsky, D. W. McBranch, C. A. Leatherdale and M. G. Bawendi, *Science*, 2000, **287**, 1011; I. Robel, R. Gresback, U. Kortshagen, R. D. Schaller and V. I. Klimov, *Phys. Rev. Lett.*, 2009, **102**, 177404.
8. W. K. Bae, Y.-S. Park, J. Lim, D. Lee, L. A. Padilha, H. McDaniel, I. Robel, C. Lee, J. M. Pietryga and V. I. Klimov, *Nat. Commun.*, 2013, **4**.
9. F. García-Santamaría, Y. Chen, J. Vela, R. D. Schaller, J. A. Hollingsworth and V. I. Klimov, *Nano Lett.*, 2009, **9**, 3482; F. García-Santamaría, S. Brovelli, R. Viswanatha, J. A. Hollingsworth, H. Htoon, S. A. Crooker and V. I. Klimov, *Nano Lett.*, 2011, **11**, 687; B. Mahler, P. Spinicelli, S. Buil, X. Quelin, J.-P. Hermier and B. Dubertret, *Nat. Mater.*, 2008, **7**, 659.
10. W. K. Bae, K. Char, H. Hur and S. Lee, *Chem. Mater.*, 2008, **20**, 531.
11. R. Vaxenburg, E. Lifshitz and A. L. Efros, *Applied Physics Letters*, 2013, **102**; J. Iveland, L. Martinelli, J. Peretti, J. S. Speck and C. Weisbuch, *Phys. Rev. Lett.*, 2013, **110**, 177406.
12. D. V. Talapin and C. B. Murray, *Science*, 2005, **310**, 86; A. Nag, M. V. Kovalenko, J.-S. Lee, W. Liu, B. Spokoynny and D. V. Talapin, *J. Am. Chem. Soc.*, 2011, **133**, 10612; A. T. Fafarman, W.-k. Koh, B. T. Diroll, D. K. Kim, D.-K. Ko, S. J. Oh, X. Ye, V. Doan-Nguyen, M. R. Crump, D. C. Reifsnyder, C. B. Murray and C. R. Kagan, *Journal of the American Chemical Society*, 2011, **133**, 15753.
13. M. Zorn, W. K. Bae, J. Kwak, H. Lee, C. Lee, R. Zentel and K. Char, *ACS Nano*, 2009, **3**, 1063.
14. J. Kwak, W. K. Bae, M. Zorn, H. Woo, H. Yoon, J. Lim, S. W. Kang, S. Weber, H.-J. Butt, R. Zentel, S. Lee, K. Char and C. Lee, *Adv. Mater.*, 2009, **21**, 5022.
15. W. K. Bae, J. Kwak, J. W. Park, K. Char, C. Lee and S. Lee, *Adv. Mater.*, 2009, **21**, 1690.

A Table of Contents Entry



Hybridization of colloidal quantum-dots and conducting polymers improves the efficiency roll-off of quantum-dot light-emitting diodes.